

## ELECTRONIC SUPPLEMENTARY INFORMATION

### Lanthanide(III)-oxamato complexes containing Nd<sup>3+</sup> and Ho<sup>3+</sup>: crystal structure, magnetic properties and *ab initio* calculations

Raphael C.A. Vaz,<sup>a</sup> Isabela O. Esteves,<sup>a</sup> Willian X.C. Oliveira,<sup>a</sup> João Honorato,<sup>b</sup> Felipe T. Martins,<sup>b</sup> Eufrânio N. da Silva Júnior,<sup>a</sup> Daniel de C. A. Valente,<sup>c</sup> Thiago M. Cardozo,<sup>c</sup> Bruno A. C. Horta,<sup>c</sup> Davor L. Mariano,<sup>d</sup> Wallace C. Nunes,<sup>e</sup> Emerson F. Pedroso,<sup>f</sup> Cynthia L.M. Pereira<sup>a\*</sup>

<sup>a</sup>Departamento de Química, Instituto de Ciências Exatas, Universidade Federal de Minas Gerais. Av. Antônio Carlos 6627, Pampulha, Belo Horizonte, Minas Gerais, 31270-901 Brazil. e-mail: [cynthialopes@ufmg.br](mailto:cynthialopes@ufmg.br)

<sup>b</sup>Instituto de Química, Universidade Federal de Goiás, Campus Samambaia Setor Itatiaia, Caixa Postal 131, Goiânia, Goiás, 74001970, Brazil;

<sup>c</sup>Instituto de Química, Universidade Federal do Rio de Janeiro, Rio de Janeiro, RJ, 21941-909, Brazil;

<sup>d</sup>Instituto de Física, Universidade Federal do Rio de Janeiro. Av. Athos da Silveira Ramos 149, Cidade Universitária, Rio de Janeiro, RJ, 24210-340, Brazil.

<sup>e</sup>Instituto de Física, Universidade Federal Fluminense, Av. Gal. Milton Tavares de Souza, s/nº, Campus da Praia Vermelha, Niterói, RJ, 24210-346, Brazil.

<sup>f</sup>Centro Federal de Educação Tecnológica de Minas Gerais, Av. Amazonas 5523, Belo Horizonte, Minas Gerais, 30421-169, Brazil.

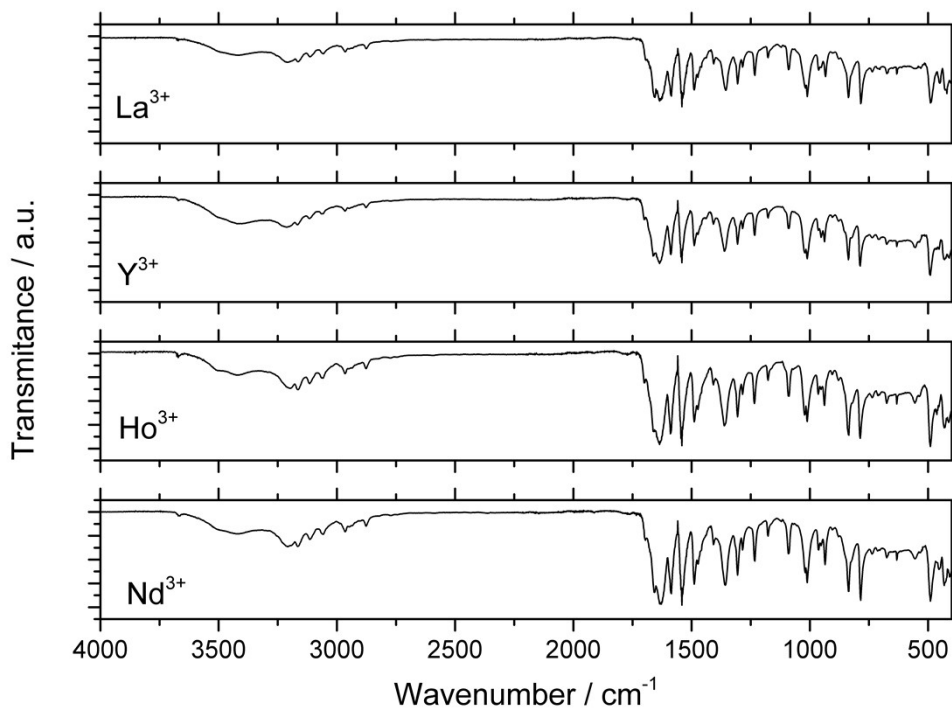


**Figure S1.** IR spectra of  $\text{La}^{3+}$ ,  $\text{Y}^{3+}$ ,  $\text{Ho}^{3+}$  and  $\text{Nd}^{3+}$  complexes containing the ligand  $_{\text{HClppa}}$ .

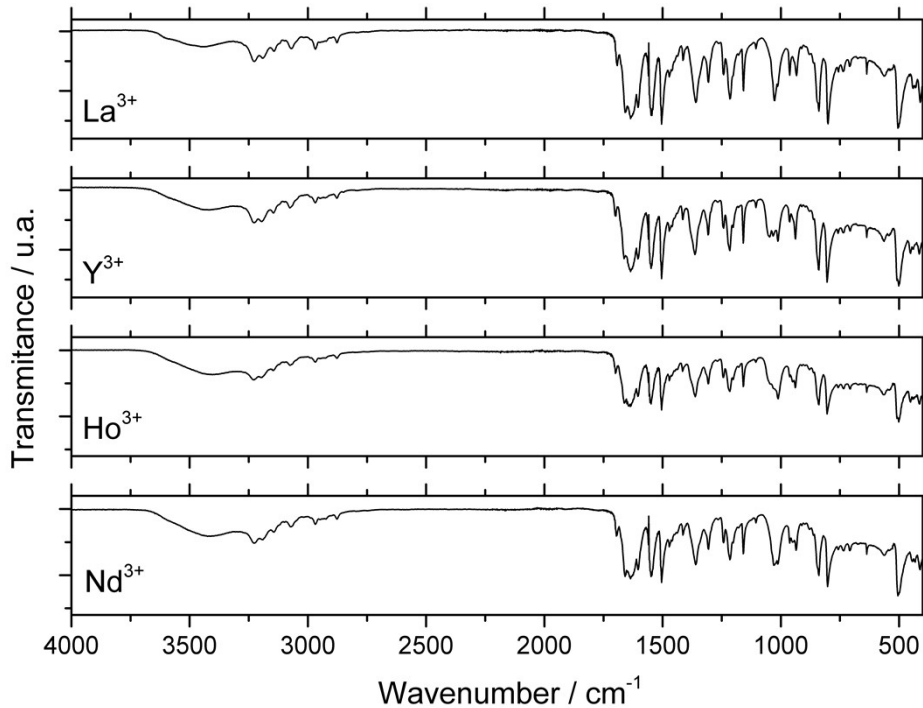


**Figure S2.** IR spectra of  $\text{La}^{3+}$ ,  $\text{Y}^{3+}$ ,  $\text{Ho}^{3+}$  and  $\text{Nd}^{3+}$  complexes containing the ligand  $_{\text{HFppa}}$ .

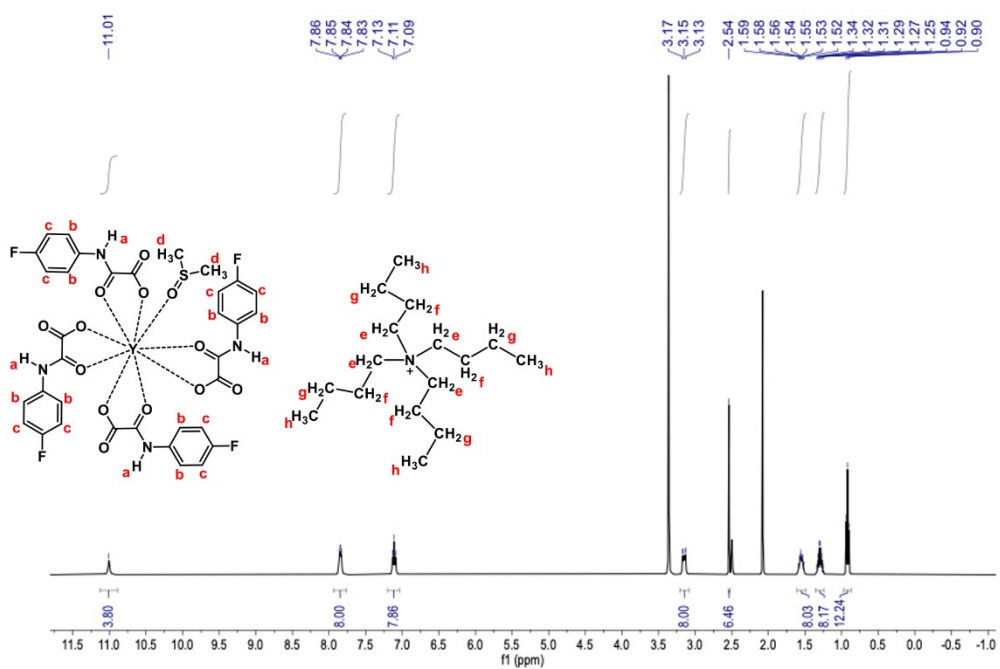


**Figure S3.** <sup>1</sup>H-NMR of compound Y\_HFppa in (CD<sub>3</sub>)<sub>2</sub>SO/(CD<sub>3</sub>)<sub>2</sub>CO (400 MHz, 25 °C).

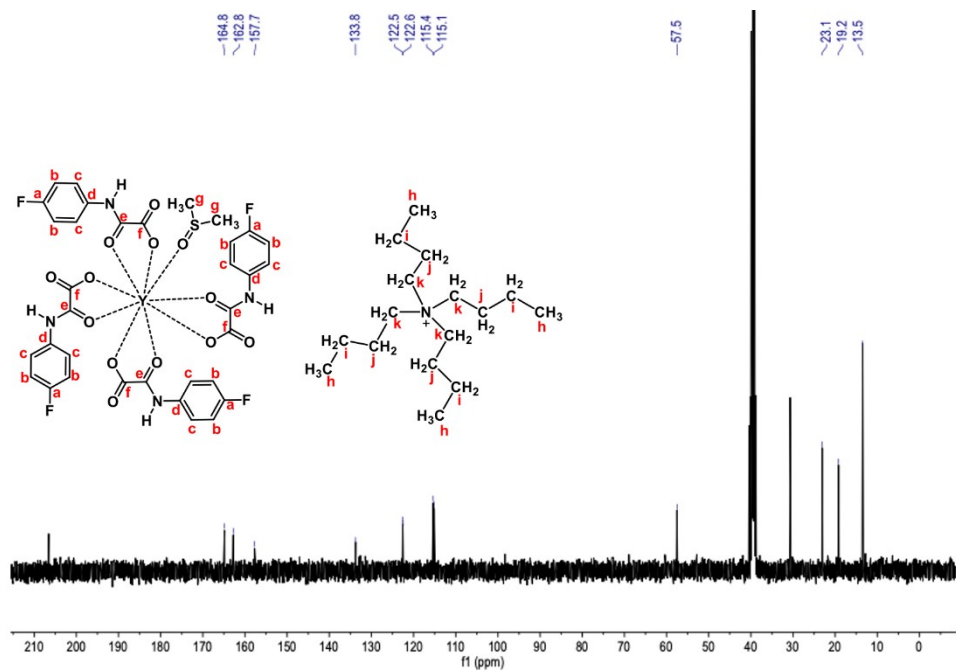


**Figure S4.** <sup>13</sup>C-NMR of compound Y\_HFppa in (CD<sub>3</sub>)<sub>2</sub>SO/(CD<sub>3</sub>)<sub>2</sub>CO (100 MHz, 25 °C).

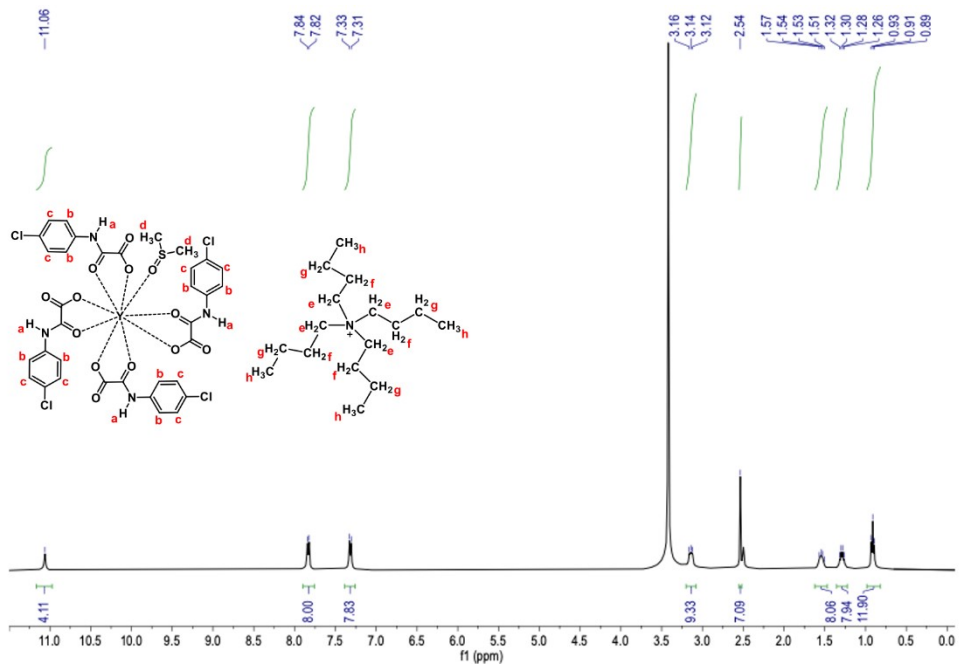


**Figure S5.**  $^1\text{H}$ -NMR of compound Y\_HClppa in  $(\text{CD}_3)_2\text{SO}$  (400 MHz, 25 °C).

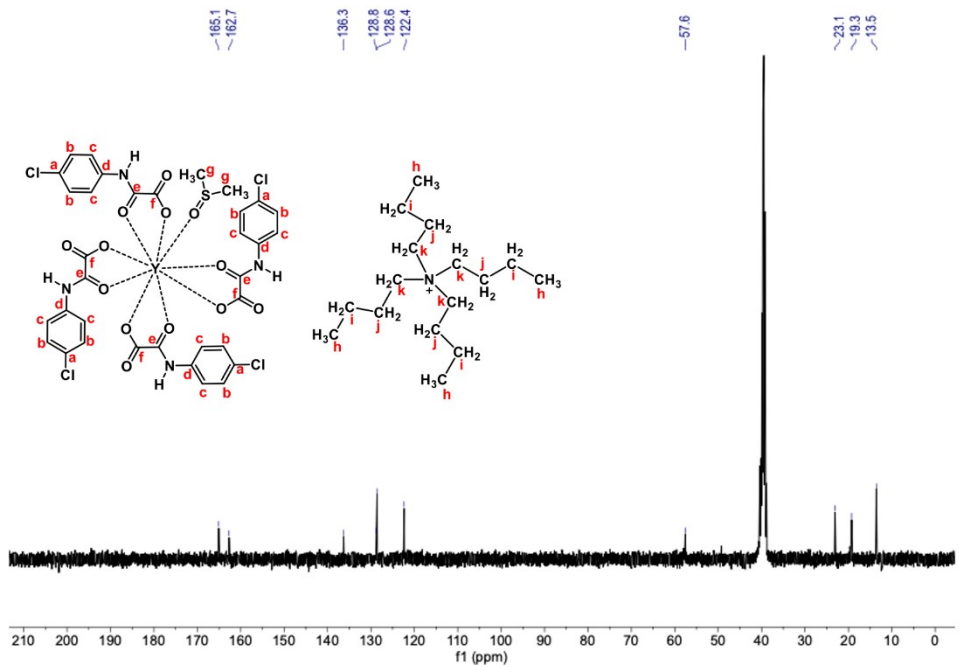


**Figure S6.**  $^{13}\text{C}$ -NMR of compound Y\_HClppa in  $(\text{CD}_3)_2\text{SO}$  (100 MHz, 25 °C).

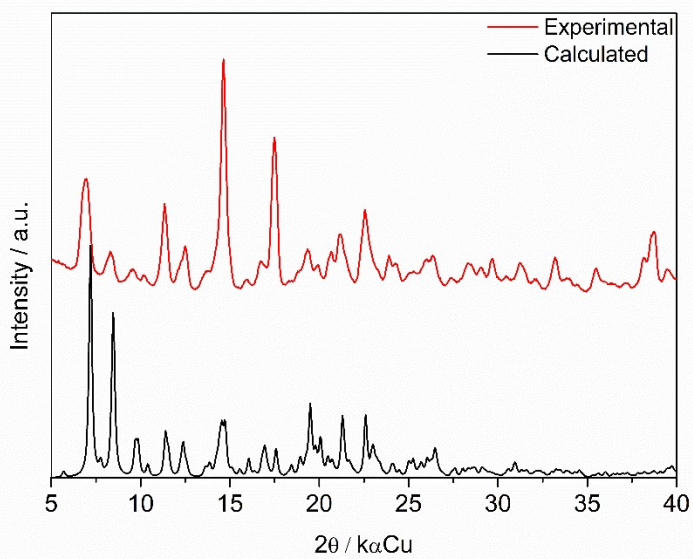


**Figure S7.** Experimental (red line) and calculated (black line) X-ray diffraction patterns for Y<sub>x</sub>H<sub>y</sub>F<sub>z</sub>ppa. The experimental pattern consists of the powder diffraction of the bulk while the calculated one consists of the simulation from single-crystal results using the Mercury® software.

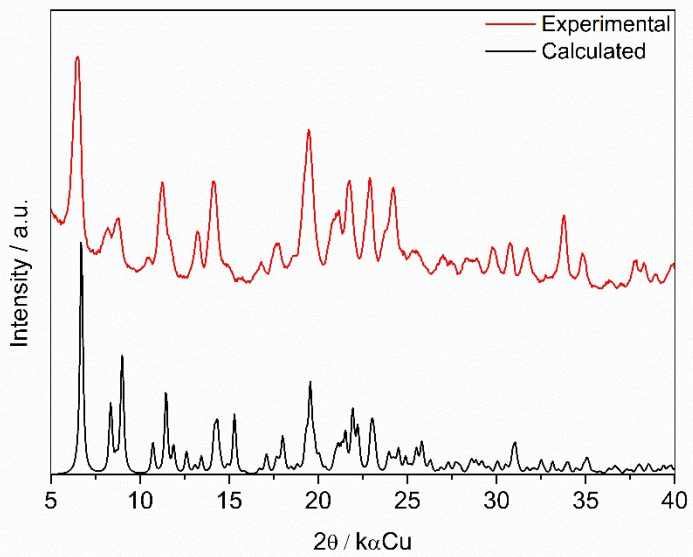


**Figure S8.** Experimental (red line) and calculated (black line) X-ray diffraction patterns for Y<sub>x</sub>H<sub>y</sub>Cl<sub>z</sub>ppa. The experimental pattern consists of the powder diffraction of the bulk while the calculated one consists of the simulation from single-crystal results using the Mercury® software.

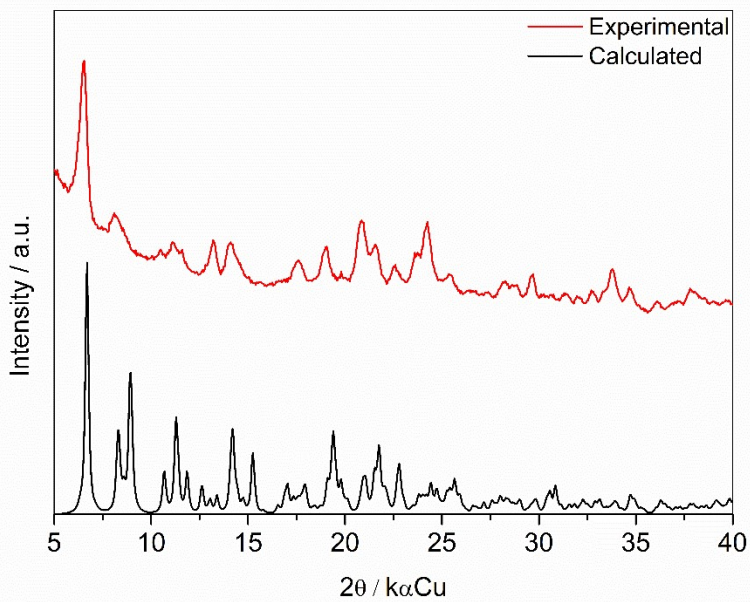


**Figure S9.** Experimental (red line) and calculated (black line) X-ray diffraction patterns for Nd\_HFppa. The experimental pattern consists of the powder diffraction of the bulk while the calculated one consists of the simulation from single-crystal results using the Mercury® software.

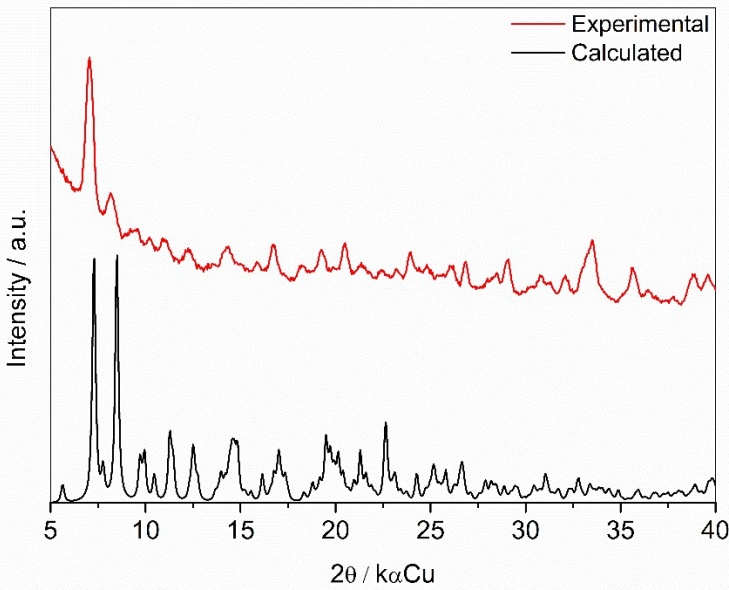


**Figure S10.** Experimental (red line) and calculated (black line) X-ray diffraction patterns for Nd\_HClppa. The experimental pattern consists of the powder diffraction of the bulk while the calculated one consists of the simulation from single-crystal results using the Mercury® software.

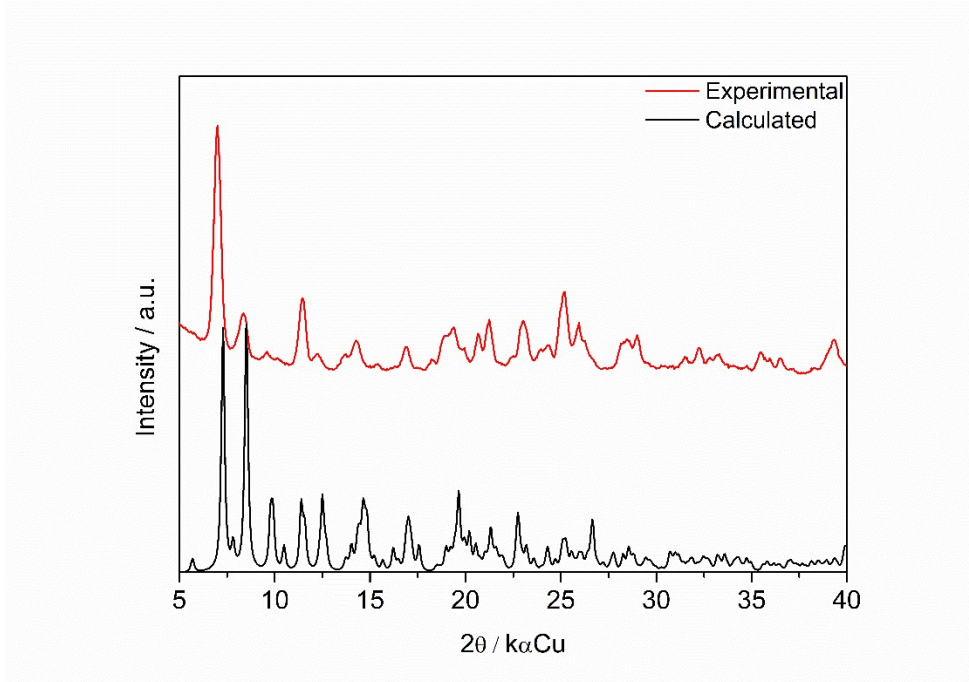


**Figure S11.** Experimental (red line) and calculated (black line) X-ray diffraction patterns for Ho\_HFppa. The experimental pattern consists of the powder diffraction of the bulk while the calculated one consists of the simulation from single-crystal results using the Mercury® software.

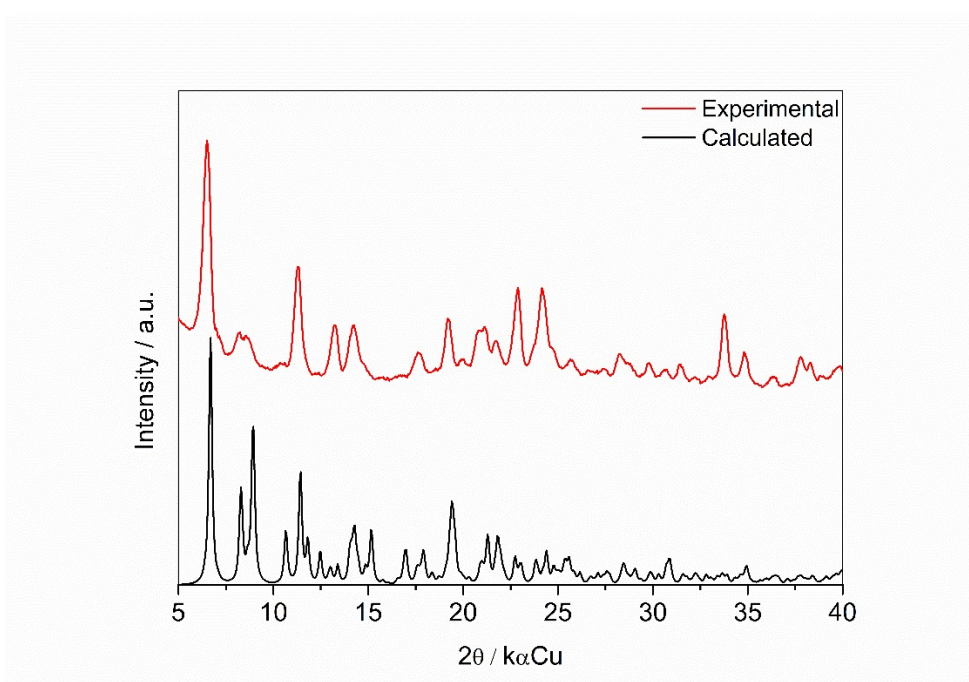


**Figure S12.** Experimental (red line) and calculated (black line) X-ray diffraction patterns for Ho\_HClppa. The experimental pattern consists of the powder diffraction of the bulk while the calculated one consists of the simulation from single-crystal results using the Mercury® software.

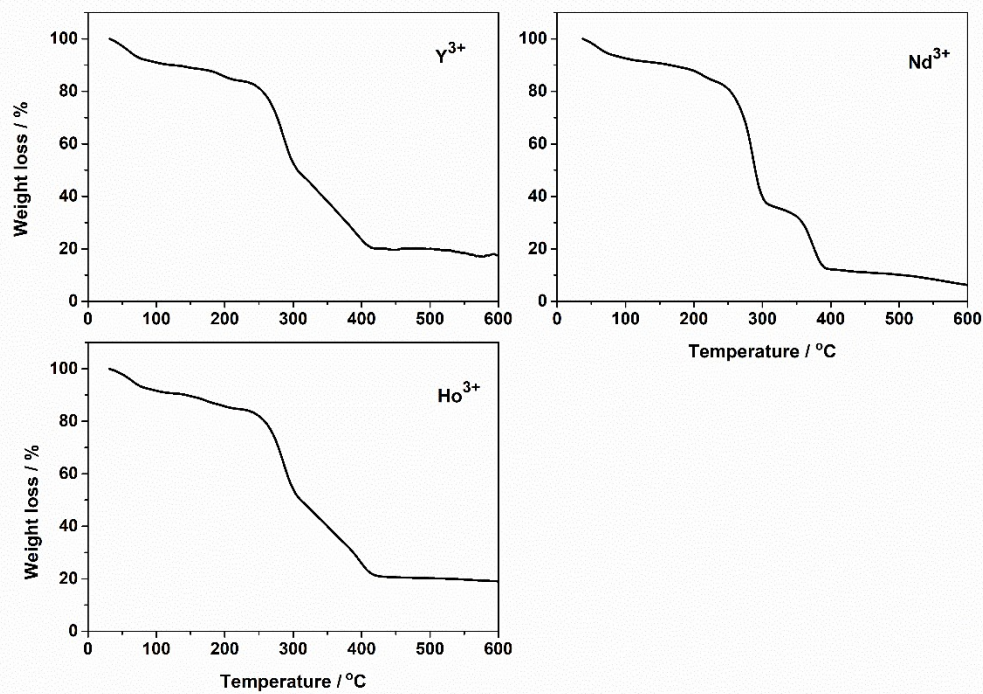


**Figure S13.** TG curves for  $Y^{3+}$ ,  $Nd^{3+}$  and  $Ho^{3+}$  compounds containing the \_HFppa ligand in the  $N_2$  atmosphere.

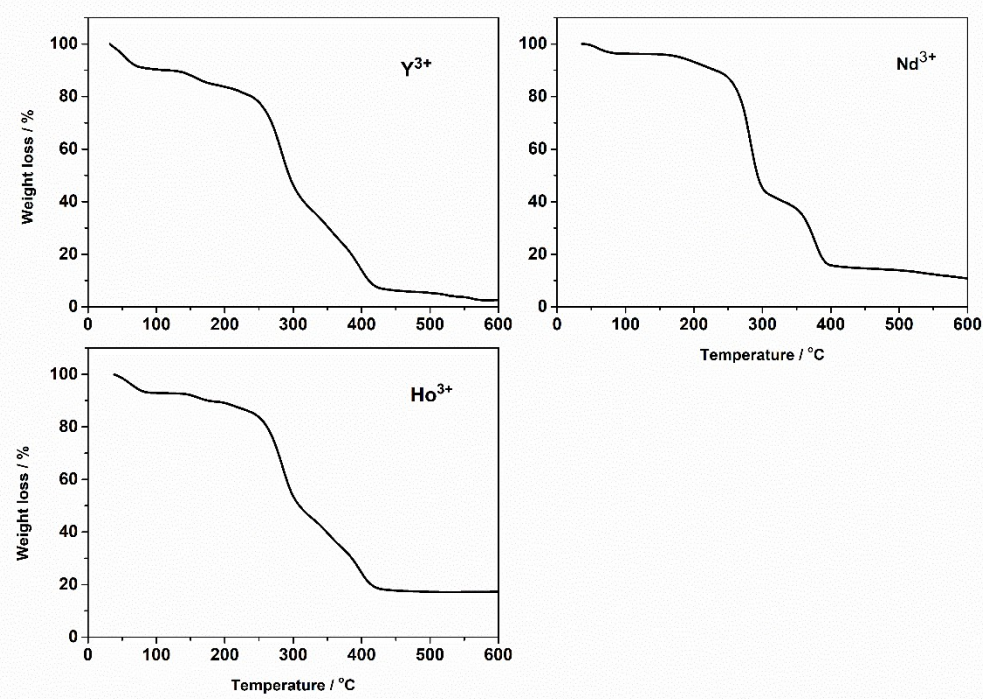


**Figure S14.** TG curves for  $Y^{3+}$ ,  $Nd^{3+}$  and  $Ho^{3+}$  compounds containing the \_HClppa ligand in the  $N_2$  atmosphere.

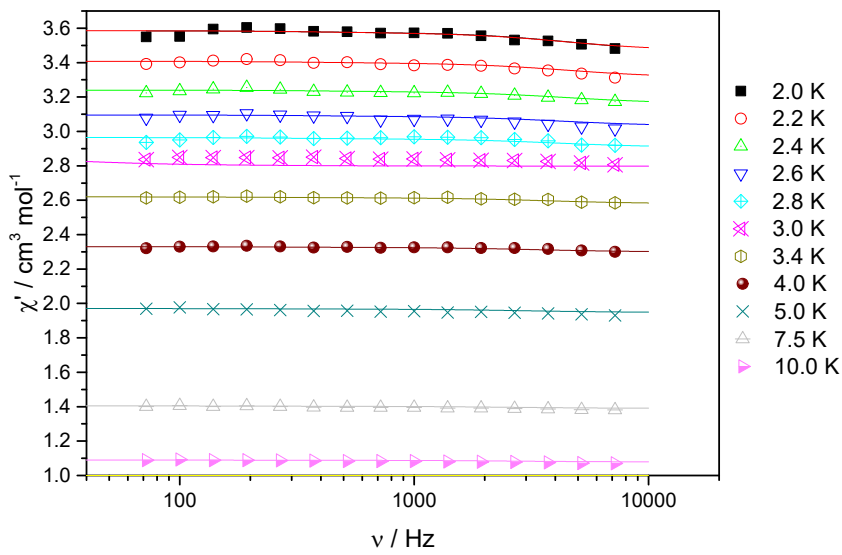


**Figure S15.** In-phase component of ac magnetic susceptibility for Ho\_HFppa complex ( $H_{dc} = 0$ ). Solid lines represent the best-fit curves according to the main text.

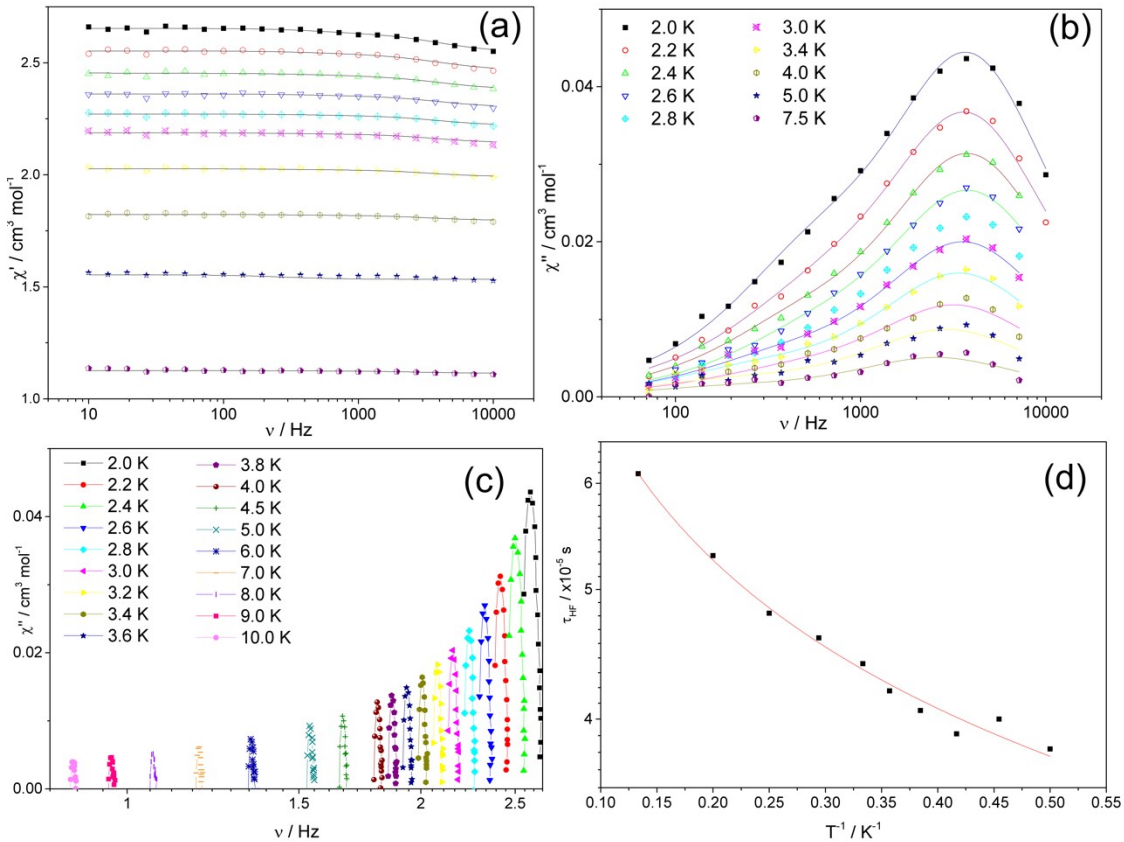


**Figure S16.** (a) In-phase and (b) out-of-phase components of ac susceptibility for Ho\_HClppa complex ( $H_{dc} = 0$ ). The solid lines are fitting with two-set of the Debye model. (c) Argand diagram constructed at fixed temperatures; lines are guides for the eyes. (d) Arrhenius plot-relaxation time vs reciprocal temperature fitted with RTB relaxation process.

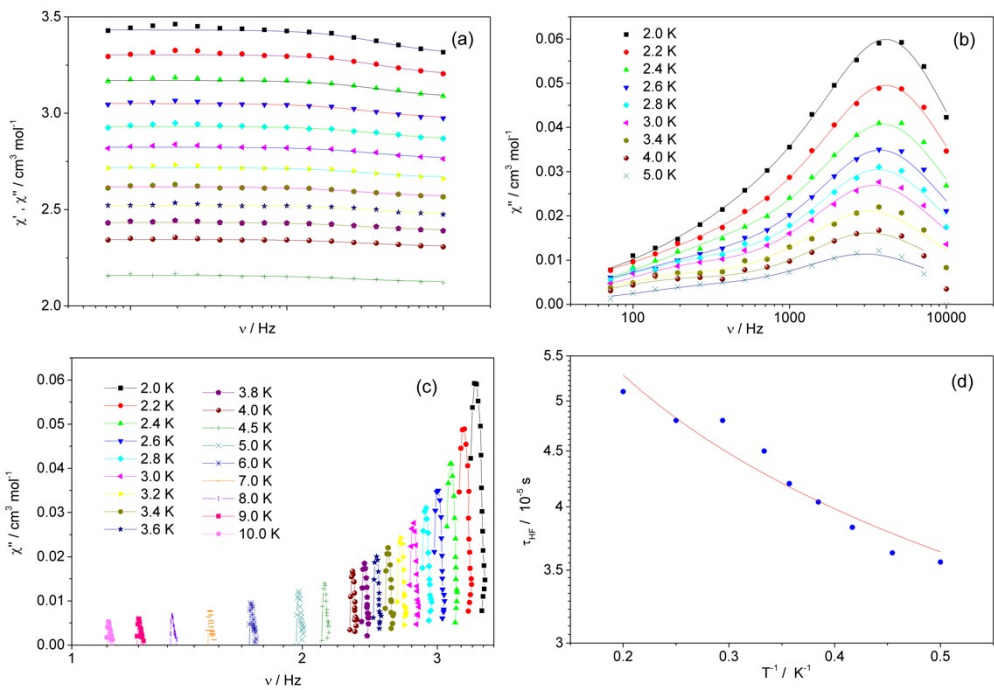


**Figure S17.** (a) In-phase and (b) out-of-phase components of ac susceptibility for Ho\_HFppa complex ( $H_{dc} = 1$  kOe). The solid lines are fitting with two-set of the Debye model. (c) Argand diagram constructed at fixed temperatures; lines are guides for the eyes. (d) Arrhenius plot-relaxation time *vs* reciprocal temperature fitted with RBT relaxation process.

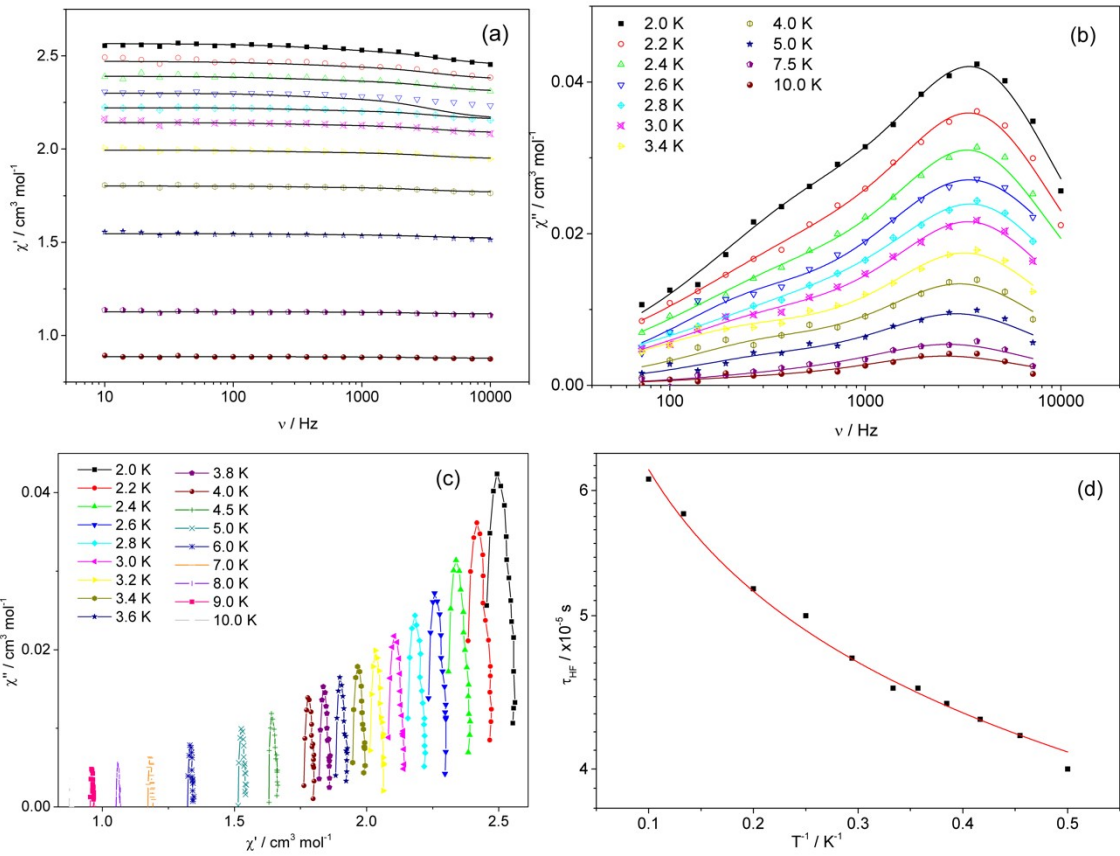


**Figure S18.** (a) In-phase and (b) out-of-phase components of ac susceptibility for Ho\_HClppa complex ( $H_{dc} = 1 \text{ kOe}$ ). The solid lines are fitting with two-set of the Debye e model. (c) Argand diagram constructed by plotting  $\chi''$  vs  $\chi'$  obtained at fixed temperatures; lines are guides for the eyes. (d) Arrhenius plot - relaxation time vs reciprocal temperature fitted with RBT relaxation process.

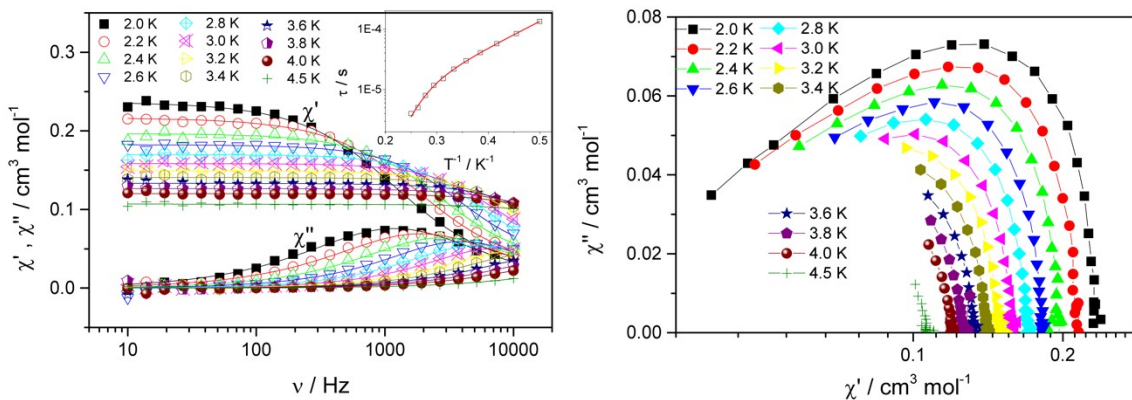


**Figure S19.** Left: In-phase and out-of-phase components of ac susceptibility for Nd\_HFppa complex ( $H_{dc} = 1 \text{ kOe}$ ). Inset: Arrhenius plot. Solid lines are the best-fit curves according to the main text—right: Argand diagram constructed by  $\chi''$  vs  $\chi'$  obtained at fixed temperatures.

**Table S1.** CShM calculations of the coordination environment at metal(III) ion in all complexes.<sup>a</sup>

Structure [ML <sub>9</sub> ]	EP-9	OPY-9	HBPY-9	JTC-9	JCCU-9	CCU-9	JCSAPR-9	CSAPR-9	JTCTPR-9	TCTPR-9	JTDIC-9	HH-9	MFF-9
La_HClppa	24.477	9.789	18.074	17.951	14.721	14.616	8.395	7.388	10.006	6.639	15.716	15.313	7.889
Y_HClppa	25.145	10.014	18.453	17.888	15.164	15.009	7.802	6.947	9.191	6.142	15.871	15.489	7.411
Nd_HClppa	24.793	9.856	18.102	18.000	14.877	14.804	8.155	7.364	9.618	6.492	15.955	15.115	7.646
Ho_HClppa	25.119	9.992	18.681	18.053	15.187	15.156	8.013	7.027	9.530	6.209	16.240	15.606	7.649
La_HFppa	29.853	19.829	20.251	17.474	11.486	12.072	7.117	7.485	6.385	8.065	15.977	13.053	7.171
Y_HFppa	29.909	19.465	20.453	17.771	11.766	12.520	6.836	7.288	6.439	8.058	16.562	13.936	6.916
Nd_HFppa	29.856	19.532	20.432	17.689	11.939	12.646	7.128	7.574	6.363	8.060	16.255	13.491	7.173
Ho_HFppa	29.763	19.421	20.570	17.933	12.166	13.026	7.187	7.723	6.537	8.320	16.728	14.061	7.265

<sup>a</sup>Abbreviations: EP-9 = Enneagon ( $D_{9h}$ ); OPY-9= Octagonal pyramid ( $C_{8v}$ ); HBPY-9 = Heptagonal bipyramid ( $D_{7h}$ ); JTC-9 = Johnson triangular cupola J3 ( $C_{3v}$ ); JCCU-9 = Capped cube J8 ( $C_{4v}$ ); CCU-9 = Spherical-relaxed capped cube ( $C_{4v}$ ); JCSAPR-9 = Capped square antiprism J10 ( $C_{4v}$ ); CSAPR-9 = Spherical capped square antiprism ( $C_{4v}$ ); JTCTPR-9 = Tricapped trigonal prism J51 ( $D_{3h}$ ); TCTPR-9 = Spherical tricapped trigonal prism ( $D_{3h}$ ); JTDIC-9 = Tridiminished icosahedron J63 ( $C_{3v}$ ); HH-9 = Hula-hoop ( $C_{2v}$ ); MFF-9 = Muffin ( $C_s$ )

**Two-set Debye model for AC susceptibility:**

a) in phase susceptibility:

$$\chi'(\omega) = \chi_S + (\chi_{T_{LF}} - \chi_S) \frac{1 + (\omega\tau_{LF})^{1-\alpha_{LF}} \sin\left(\frac{\pi\alpha_{LF}}{2}\right)}{1 + 2(\omega\tau_{LF})^{1-\alpha_{LF}} \sin\left(\frac{\pi\alpha_{LF}}{2}\right) + (\omega\tau_{LF})^{2-2\alpha_{LF}}} + (\chi_{T_{HF}} - \chi_{T_{LF}})$$

b) out-of-phase susceptibility:

$$\chi'(\omega) = (\chi_{T_{LF}} - \chi_S) \frac{1 + (\omega\tau_{LF})^{1-\alpha_{LF}} \cos\left(\frac{\pi\alpha_{LF}}{2}\right)}{1 + 2(\omega\tau_{LF})^{1-\alpha_{LF}} \sin\left(\frac{\pi\alpha_{LF}}{2}\right) + (\omega\tau_{LF})^{2-2\alpha_{LF}}} + (\chi_{T_{HF}} - \chi_{T_{LF}})$$

**Table S2.** Parameters of two-set Debye model for Ho\_HFppa complex.

<b>H<sub>dc</sub> = 0</b>							
<b>T / K</b>	$\chi_S$	$\chi_{T_{LF}}$	$\chi_{T_{HF}}$	$\alpha_{LF}$	$\alpha_{HF}$	$\tau_{LF}/10^{-4}s$	$\tau_{HF}/10^{-5}s$
2.0	3.465(3)	3.476(8)	3.5853(5)	0.00(19)	0.04(4)	4.5(16)	3.46(11)
2.2	3.3140(19)	3.324(5)	3.4077(5)	0.00(12)	0.00(3)	4.4(20)	3.55(8)
2.4	3.1630(3)	3.172(8)	3.2400(4)	0.0(2)	0.00(5)	3.7(17)	3.58(16)
2.6	3.0320(6)	3.0399(6)	3.0956(5)	0.00(16)	0.00(4)	4.3(14)	3.76(14)
2.8	2.908(3)	2.916(7)	2.9646(6)	0.0(3)	0.00(8)	5.4(28)	3.9(2)
3.0	2.7988(16)	2.804(5)	2.8474(7)	0.0(2)	0.00(6)	5.0(20)	4.1(2)
3.4	2.5802(7)	2.5856(6)	2.6198(7)	0.0(3)	0.00(6)	6.8(27)	4.4(2)
4.0	2.2895(8)	2.3037(8)	2.3299(8)	0.00(15)	0.00(2)	5.3(19)	4.8(3)
5.0	1.948(2)	1951(7)	1.970(2)	0.0(8)	0.00(19)	6(8)	5.4(12)
7.5	1.3905(15)	1.393(5)	1.405(3)	0.0(10)	0.00(19)	7(5)	6.1(6)
10.0	1.0788(13)	1.080(4)	1.089(4)	0.0(12)	0.0(2)	7(13)	6(2)
<b>H<sub>dc</sub> = 1 kOe</b>							
<b>T / K</b>	$\chi_S$	$\chi_{T_{LF}}$	$\chi_{T_{HF}}$	$\alpha_{LF}$	$\alpha_{HF}$	$\tau_{LF}/10^{-4}s$	$\tau_{HF}/10^{-5}s$
2.0	3.295(4)	3.341(3)	3.443(3)	0.28(13)	0.00(6)	2.2(22)	3.56(21)
2.2	3.194(4)	3.229(19)	3.318(2)	0.32(17)	0.00(5)	3(3)	3.63(16)
2.4	3.132(2)	3.154(3)	3.181(2)	0.16(20)	0.00(5)	5(2)	3.8(2)
2.6	2.974(2)	2.992(8)	3.058(3)	0.2(2)	0.00(5)	6(3)	4.0(2)
2.8	2.871(2)	2.885(2)	2.944(2)	0.2(3)	0.00(8)	7(6)	4.2(2)
3.0	2.769(2)	2.780(2)	2.833(3)	0.0(4)	0.00(12)	8(2)	4.5(2)
3.4	2.570(3)	2.579(6)	2.620(5)	0.0(4)	0.00(8)	9(5)	4.8(5)
4.0	2.307(4)	2.315(4)	2.347(5)	0.0(3)	0.00(7)	9(3)	4.8(3)
5.0	1.971(2)	1.976(4)	1.998(3)	0.0(3)	0.00(9)	6(3)	5.1(5)
7.5	1.515(2)	1.517(5)	1.531(3)	0.0(9)	0.00(17)	6(9)	5.7(13)
10.0	1.225(5)	1.227(6)	1.237(7)	0.0(10)	0.0(2)	6(9)	5.8(19)

**Table S3.** Parameters of two-set Debye model for Ho<sub>2</sub>HClppa.

<b>H<sub>dc</sub> = 0</b>							
<b>T / K</b>	$\chi_S$	$\chi_{T_{LF}}$	$\chi_{T_{HF}}$	$\alpha_{LF}$	$\alpha_{HF}$	$\tau_{LF}/10^{-4}s$	$\tau_{HF}/10^{-5}s$
2.0	2.546(2)	2.578(2)	2.654(2)	0.14(9)	0.00(5)	2.3(12)	3.8(3)
2.2	2.468(2)	2.484(9)	2.553(8)	0.05(15)	0.00(5)	3.2(14)	4.0(3)
2.4	2.383(2)	2.398(2)	2.454(3)	0.17(14)	0.00(6)	2.6(19)	3.9(3)
2.6	2.302(2)	2.311(8)	2.362(3)	0.05(17)	0.00(6)	3.0(17)	4.0(3)
2.8	2.221(2)	2.227(9)	2.271(8)	0.0(4)	0.00(9)	3.6(11)	4.2(2)
3.0	2.143(2)	2.148(9)	2.187(9)	0.0(2)	0.00(6)	4.8(18)	4.4(2)
3.4	1.991(2)	1.986(4)	2.027(5)	0.0(2)	0.00(5)	6(3)	4.6(3)
4.0	1.796(2)	1.800(6)	1.823(6)	0.0(5)	0.00(12)	5(5)	4.8(7)
5.0	1.534(2)	1.537(6)	1.554(5)	0.0(5)	0.00(15)	8(4)	5.3(4)
7.5	1.115(2)	1.116(4)	1.126(4)	0.0(19)	0.00(18)	9(11)	6.1(14)

<b>H<sub>dc</sub> = 1 kOe</b>							
<b>T / K</b>	$\chi_S$	$\chi_{T_{LF}}$	$\chi_{T_{HF}}$	$\alpha_{LF}$	$\alpha_{HF}$	$\tau_{LF}/10^{-4}s$	$\tau_{HF}/10^{-5}s$
2.0	2.450(2)	2.496(14)	2.5662(7)	0.18(9)	0.00(6)	3.5(12)	4.0(3)
2.2	2.373(2)	2.411(16)	2.471(2)	0.24(14)	0.00(7)	4(2)	4.2(2)
2.4	2.308(2)	2.337(12)	2.391(9)	0.19(16)	0.00(7)	5(2)	4.3(4)
2.6	2.225(3)	2.239(8)	2.299(9)	0.00(18)	0.09(7)	6.7(17)	4.4(3)
2.8	2.159(2)	2.181(2)	2.221(3)	0.0(2)	0.00(5)	6(3)	4.5(2)
3.0	2.086(2)	2.103(5)	2.142(4)	0.14(12)	0.00(5)	5.6(17)	4.4(2)
3.4	1.948(2)	1.962(5)	1.995(4)	0.10(18)	0.00(7)	7(2)	4.7(3)
4.0	1.769(2)	1.776(6)	1.801(6)	0.00(13)	0.0(3)	6(3)	5.0(7)
5.0	1.522(2)	1.527(5)	1.545(6)	0.0(3)	0.00(13)	6(4)	5.2(8)
7.5	1.115(2)	1.116(5)	1.127(4)	0.0(12)	0.00(19)	5(12)	5.8(18)
10.0	0.878(5)	0.879(8)	0.886(8)	0.0(14)	0.00(19)	7(14)	6.1(16)

**Table S4.** Cole-Cole parameters were obtained from fits of the frequency-dependence of ac susceptibility for Nd<sub>2</sub>HClppa using the generalized Debye model. (H<sub>dc</sub> = 1 kOe)

T(K)	$\chi_S$ (emu/K)	$\chi_T$ (emu/K)	$\alpha$	$\tau$ (s)
2.0	0.010(4)	0.1187(5)	0.288(6)	7,62(11)x10 <sup>-4</sup>
2.2	0.0092(8)	0.0959(8)	0.262(14)	4,76(15)x10 <sup>-4</sup>
2.4	0.0076(6)	0.0825(5)	0.274(10)	3,26(8)x10 <sup>-4</sup>
2.6	0.0074(7)	0.0696(4)	0.248(12)	2,14(6)x10 <sup>-4</sup>
2.8	0.0073(7)	0.0599(4)	0.224(14)	1,47(5)x10 <sup>-4</sup>
3.0	0.0069(9)	0.0526(4)	0.211(18)	1,03(4)x10 <sup>-4</sup>
3.2	0.0069(7)	0.0459(2)	0.185(15)	0,73(2)x10 <sup>-4</sup>
3.4	0.0071(6)	0.0405(2)	0.154(14)	0,53(2)x10 <sup>-4</sup>
3.6	0.0068(10)	0.0362(2)	0.147(9)	0,39(2)x10 <sup>-4</sup>
3.8	0.0068(11)	0.0323(2)	0.124(2)	0,29(2)x10 <sup>-4</sup>
4.0	0.0059(14)	0.0295(2)	0.14(3)	0,21(2)x10 <sup>-4</sup>
4.5	0.0053(19)	0.0232(10)	0.14(3)	0,11(2)x10 <sup>-4</sup>

**Table S5.** Cole-Cole parameters were obtained from fits of the frequency-dependence of ac susceptibility for Nd<sub>2</sub>HFppa using the generalized Debye model. ( $H_{dc} = 1$  kOe)

T(K)	$\chi_s$ (emu/K)	$\chi_T$ (emu/K)	$\alpha$	$\tau$ (s)
2.0	0.0106(10)	0.1185(5)	0.221(9)	1.34(3)x10 <sup>-4</sup>
2.2	0.0106(10)	0.0985(4)	0.211(9)	8.41(19)x10 <sup>-5</sup>
2.4	0.0127(13)	0.0820(4)	0.166(15)	3.26(8)x10 <sup>-5</sup>
2.6	0.0138(15)	0.0702(3)	0.134(19)	4.08(19)x10 <sup>-5</sup>
2.8	0.0141(10)	0.0607(2)	0.112(14)	2.98(10)x10 <sup>-5</sup>
3.0	0.0138(10)	0.0528(13)	0.095(14)	2.18(9)x10 <sup>-5</sup>
3.2	0.0119(16)	0.0467(12)	0.106(19)	1.52(10)x10 <sup>-5</sup>
3.4	0.0121(14)	0.04141(8)	0.094(17)	1.17(8)x10 <sup>-5</sup>
3.6	0.011(4)	0.03701(15)	0.11(5)	0.8(2)x10 <sup>-5</sup>
3.8	0.007(8)	0.03333(13)	0.15(5)	0.5(2)x10 <sup>-5</sup>
4.0	0.008(8)	0.03003(10)	0.14(6)	0.4(2)x10 <sup>-5</sup>
4.5	0.010(9)	0.02373(7)	0.15(9)	0.3(3)x10 <sup>-5</sup>

**Table S6.** 18 lowest energy levels of Ln\_HXppa compounds (Ln = Ho, Nd and X = F, Cl), in cm<sup>-1</sup>. These are the SO-RASSI energies, based on the CASSCF calculations specified in the Computational Details section.

State	Compound			
	Nd		Ho	
	_HFppa	_HClppa	_HFppa	_HClppa
1	0.0	0.0	0.0	0.0
2	0.0	0.0	5.0	1.6
3	22.6	34.3	32.7	36.4
4	22.6	34.3	45.1	42.0
5	195.9	198.3	96.8	74.2
6	195.9	198.3	146.8	129.8
7	302.9	311.6	156.6	144.2
8	302.9	311.6	159.9	152.9
9	323.8	342.7	169.8	157.6
10	323.8	342.7	176.5	163.6
11	2042.5	2048.9	196.2	186.5
12	2042.5	2048.9	207.4	192.6
13	2076.4	2088.9	265.3	241.9
14	2076.4	2088.9	273.5	243.6
15	2158.3	2163.3	300.5	282.5
16	2158.3	2163.3	306.1	295.8
17	2174.4	2186.1	311.3	299.2
18	2174.4	2186.1	5329.1	5326.2

**Table S7.** Crystal-field parameters ( $B_k^q$ , cm $^{-1}$ ) obtained from ab initio calculations for the Ln\_HXppa (Ln = Ho, Nd and X = F, Cl) compound. Only an upper limit for the norm of parameters of rank  $k \geq 8$  was included.

Rank of parameters		Compound			
$k$	$q$	Nd		Ho	
		F	Cl	F	Cl
2	-2	1.84E+00	-2.08E+00	4.16E-03	1.51E-02
	-1	2.16E+00	-2.40E+00	-5.37E-02	-2.49E-02
	0	-1.05E+00	-8.65E-01	4.40E-01	-3.38E-01
	1	2.09E+00	8.91E-02	1.14E-01	2.30E-01
	2	-4.41E-01	-8.42E-01	-3.83E-01	1.99E-02
4	-4	4.00E-02	-4.11E-02	5.28E-03	2.61E-03
	-3	-8.28E-02	-1.07E-01	-4.01E-03	-6.76E-04
	-2	9.20E-02	-1.06E-01	-6.75E-04	4.21E-03
	-1	1.06E-02	1.63E-02	2.37E-03	-2.55E-03
	0	1.13E-02	1.00E-02	-8.69E-04	8.37E-04
	1	5.09E-04	2.51E-02	3.98E-04	2.99E-03
	2	-4.10E-02	-5.59E-02	-3.98E-04	-5.39E-03
	3	1.49E-01	9.01E-02	-2.47E-04	-2.59E-04
	4	3.48E-02	4.40E-02	9.97E-03	-4.61E-05
6	-6	7.62E-03	5.12E-03	5.14E-05	-2.29E-04
	-5	-3.15E-02	-1.30E-02	5.02E-04	9.32E-04
	-4	9.01E-03	-6.63E-03	3.39E-05	1.89E-04
	-3	5.30E-03	8.65E-03	3.06E-04	-2.20E-04
	-2	3.94E-03	2.59E-03	8.25E-07	-2.81E-05
	-1	-8.16E-04	8.31E-03	6.55E-05	-6.81E-05
	0	1.10E-03	1.07E-03	-6.54E-06	3.01E-05
	1	-1.04E-02	9.21E-03	6.02E-05	2.27E-04
	2	5.87E-03	-5.90E-03	-5.72E-05	-5.03E-05
	3	1.37E-02	8.82E-03	1.11E-04	2.21E-04
	4	5.12E-03	7.39E-03	-4.26E-04	4.45E-06
	5	-3.84E-02	5.78E-02	-1.63E-04	4.24E-04
	6	-8.79E-03	-9.11E-03	2.02E-04	-1.23E-04
8 (Nd) 8-12 (Ho)		< 4.54E-04	< 5.50E-04	< 1.04E-07	< 1.00E-07